Endocrine (2019) 66:585–595
https://doi.org/10.1007/s12020-019-02048-y

ORIGINAL ARTICLE

Check for updates

miR-762 modulates thyroxine-induced cardiomyocyte hypertrophy by inhibiting Beclin-1

Zheng Qiang[1] · Beifang Jin[1] · Yuntao Peng[1] · Yan Zhang[1] · Junfeng Wang[1] · Chen Chen[1] · Xinfeng Wang[1] · Fang Liu[1,2]

Received: 14 May 2019 / Accepted: 5 August 2019 / Published online: 14 September 2019

Abstract

Purpose Whether autophagy plays a key role in thyroxine-induced cardiomyocyte hypertrophy, and whether the role of autophagy in thyroxine-induced cardiomyocyte hypertrophy is related to targeting of Beclin-1 by miR-762 remains unclear. This research focused on testing these two hypotheses. Importantly, the results of this study will help us better understand the molecular mechanisms of thyroxine-induced cardiomyocyte hypertrophy.

Methods In vivo and in vitro, RT-PCR, western blot, and dual luciferase reporter assay were performed to understand the molecular mechanism of thyroxine-induced cardiomyocyte hypertrophy. HE staining, Masson staining, transmission electron microscopy, and immunofluorescence were used to observe intuitively changes of hearts and cardiomyocytes.

Results Our results showed that in vivo, serum TT3, TT4, and heart rate were significantly upregulated in the T4 group compared with the control group. Moreover, the surface area of cardiomyocytes was significantly increased in the T4 group, and the structural disorder was accompanied by obvious hyperplasia of collagen fibers. The expression of ANP, and β-MHC was significantly upregulated in the T4 group. In addition, LC3 II/LC3 I, Beclin-1 and the count of autophagic vacuoles were significantly upregulated, but miR-762 was significantly downregulated in the T4 group compared to the control group. Subsequently, a dual luciferase reporter assay suggested that Beclin-1 was the target gene of miR-762. In vitro, the results for the T3 group were consistent with the results for the T4 group. Furthermore, cardiomyocyte hypertrophy and autophagic activity were attenuated in the T3 + miR-762 mimic group compared with the T3 group. In contrast, cardiomyocyte hypertrophy and autophagic activity were aggravated in the T3 + miR-762 inhibitor group compared with the T3 group.

Conclusions miR-762 modulates thyroxine-induced cardiomyocyte hypertrophy by inhibiting Beclin-1.

Keywords miR-762 · Beclin-1 · Autophagy · Thyroxine · Cardiomyocyte hypertrophy

Introduction

Hyperthyroidism is a common endocrine diseases that affects 1.2% of the population in the United States [1]. The causes include Graves' disease, inflammatory hyperthyroidism, drug-induced hyperthyroidism, human chorionic gonadotropin-related hyperthyroidism, and TSH pituitary tumor- and toxic thyroid adenoma- related hyperthyroidism [2], and Graves' disease accounts for 50–80% of all causes [3]. Hyperthyroidism is 8–10 times more likely to occur in women than in men, and onset usually occurs between the age of 20 and 50 years [2]. Excessive thyroxine can cause direct or indirect toxicity to the heart and lead to cardiomyocyte hypertrophy (thyroxine-induced cardiomyocyte hypertrophy) [4]. However, thyroxine-induced cardiomyocyte hypertrophy is only a compensatory response to injury that manifests as an increase in the size of cardiomyocytes, without an increase in the number of cardiomyocytes. At the initial stage of compensation, cardiac output can remain relatively normal. If the cause is not eliminated for a long time, it leads to ventricular dilatation, contractile dysfunction, and cardiomyocyte fibrosis, and eventually to chronic heart failure [5].

✉ Zheng Qiang
qiangzheng521@outlook.com

✉ Fang Liu
fang.liu@msn.com

[1] Department of Anatomy, Guilin Medical University, 541004 Guilin, China

[2] Center of Diabetic Systems Medicine, Guangxi Key Laboratory of Excellence, Guilin Medical University, 541004 Guilin, China

Autophagy is a highly conserved catabolic process in which damaged organelles and proteins are cleared by lysosomes, and then the product is reused to maintain cellular homeostasis [6]. Autophagy is divided into three forms: microautophagy, macroautophagy and chaperone-mediated autophagy (CMA), whose mechanisms of transmission to lysosomes differ. Microautophagy is a process in which lysosomes directly absorb and degrade damaged organelles and proteins [7]. In CMA, damaged organelles and proteins have a pentapeptide sequence that binds to the heat shock protein HSP70 to form a substrate-chaperone complex, which is recognized by lysosomal surface receptors, and then transmitted to lysosomes for degradation after being folded [8]. Thus far, most studies have focused on macroautophagy. Macroautophagy proceeds as follows [9]: (1) Cells receive an autophagy signal; (2) the endoplasmic reticulum forms vesicles; (3) the vesicles wrap the damaged organelles or proteins to form autophagic vacuoles; (4) lysosomes degrade the autophagic vacuoles; and5. the product is reused by the cytoplasm, and the residues are expelled from the cell.

MicroRNAs (miRNAs, miRs) are a class of endogenous noncoding RNAs that are involved in the regulation of 30–50% of gene expression [10]. miRNAs modulate gene expression at the posttranscriptional level by binding to seed-matched sequences in the 3′-UTR regions of target mRNAs [11].

Autophagy, described above, plays key roles in atherosclerosis, myocardial infarction, heart failure, and other cardiovascular diseases [12–14]. Therefore, we hypothesized that autophagy may also play a key role in thyroxine-induced cardiomyocyte hypertrophy. Moreover, recent research has found that miR-762 is significantly upregulated in the plasma of Graves' disease patients [15]. Interestingly, we found that several nucleotides of miR-762 are perfectly complementary to the 3′-UTR region of the autophagy related gene Beclin-1 in mice. Thus, we also hypothesized that the role of autophagy in thyroxine-induced cardiomyocyte hypertrophy is related to targeting of Beclin-1 by miR-762. This research focused on testing these two hypotheses. Importantly, this study will help us better understand the molecular mechanisms of thyroxine-induced cardiomyocyte hypertrophy.

Materials and methods

Thyroxine

The thyroid secretes thyroxines including T3 and T4. Both molecules can generate biological activity by binding to thyroid hormone receptors. The vast majority of T3 is transformed from T4 by deiodination. The affinity of thyroid hormone receptors for T3 is approximately tenfold higher than that for T4. Therefore, T4 must be converted into T3 to pto produce an electrocardiogramroduce potent thyroid hormone receptor-mediated effects [16]. However, T4 can also act directly through thyroid hormone receptors and its molecular structure is more stable than that of T3 [17]. Therefore, in vivo, mice were intraperitoneally injected with T4 (Sigma-Aldrich, T2376) solution, and in vitro, the cardiomyocytes were stimulated with T3 (Sigma-Aldrich, T2877) solution.

Animals and treatment

Male C57BL/6J mice ($n = 60$) that were 8 weeks old purchased from the Hunan SiLaikeJingda Experimental Animals Company Limited under license number SCXK (xiang) 2016-0002. The environment was maintained at ~24 °C, and the mice were given free access to a basal diet. All mice were allowed to acclimate to the food for 1 week. At the 9th week, the mice were randomly divided into a control group ($n = 30$) and a T4 group ($n = 30$). The T4 group was intraperitoneally injected with T4 solution at 1 μg/g, and the control group was intraperitoneally injected with 150 μl of normal saline. The intraperitoneal injections were given every 48 h for 7 weeks until the 16th week. The stock-solution contained 2 mg/ml T4 dissolved in 0.01 M NAOH with 0.1% BSA (Solarbio, A8010). T4 solution was stock-solution diluted 1:10 with normal saline. The T4 solutions (stock and diluted) were prepared fresh every 2 weeks and kept protected from light at 4 °C. All animal protocols were approved by the review board of the Animal Care and Ethics Committee of Guilin Medical University.

Electrocardiogram

The mice were anesthetized with 10% chloral hydrate and fixed on the table. Silver needle electrodes were inserted into the limbs: red-left hand; white-right hand; and black-left foot. An electrocardiograph (TECHMAN, BL-420S) was used to produce an electrocardiogram.

ELISA

At the 16th week, blood samples were collected from the retrobulbar venous plexus with a micropipette and left at room temperature for 30 min. Serum samples were obtained by centrifugation for 15 min at 6000 rpm and stored at −80 °C. Commercial ELISA kits (CUSABIO, CSB-E05086m and CSB-E05083m) were used to measure TT3 and TT4 concentrations. Serum sample with known thyroxine concentrations were used as standards.

Table 1 Sequences for primers

Gene	RT-PCR
miR-762	5-GTCGTATCCAGTGCGTGTCGTGGAGTCGGCAATTGCACTGGATACGAC GCTCTGTCC-3
U6	5-AACGCTTCACGAATTTGCGT-3

Morphology

Heart samples were washed and immersed in 4% paraformaldehyde for 24 h. The hearts were then washed in gradient alcohols, clear with xylene and embedded in paraffin. The paraffin-embedded hearts were cut into slices of 5 μm for HE, and Masson staining (Solarbio, G1120 and G1340). Upon microscopic observation, the cell nuclei were purple, the cytoplasm was pink, the cardiomyocyte fibers were red, and the collagen fiber were blue. Quantitative analysis of cell surface area and collagen fiber proportions was performed using ImageJ software. Microscopy (OLYMPUS, BX53) was performed at magnifications of ×200 and ×400.

Real-Time PCR

Total RNA extraction and cDNA synthesis: Total RNA was extracted from hearts or cardiomyocytes using the TRIzol (Thermo, 10296010) method. Using a spectrophotometer the RNA purity and concentration were detected. One microgram of RNA was reverse transcribed into cDNA with a reverse transcription kit (TOYOBO, FSQ-201). The cDNA was diluted ten times with nuclease-free water. Real-time fluorescent quantitative PCR: Real-time PCR was performed in a 20 μl system with 10 μl of SYBR^{TM} Green Master mix (Applied Biosystems, 4364346), 7 μl of nuclease-free water, 1.4 μl of cDNA, 0.8 μl of forward primer, and 0.8 μl of reverse primer. The reaction condition: 50 °C for 20 s and 95 °C for 10 min followed by 40 cycles of 95 °C for 15 s and 60 °C for 60 s in an Applied Biosystems 7500 Real-Time PCR System. U6 was used as an internal reference with the $2^{-\Delta\Delta CT}$ method to calculate relative miR-762 expression. GAPDH was used as an internal reference with the $2^{-\Delta\Delta CT}$method to calculate relative ANP, β-MHC and Beclin-1 expression. All primers (Invitrogen) are shown in Tables 1 and 2.

Western blot analysis

The hearts and cardiomyocytes were fully homogenized in RIPA Lysis Buffer (Solarbio, R0010) and PMSF (Solarbio, P0100). The proteins were obtained by centrifugation and boiled in the SDS-PAGE loading buffer for 10 min. SDS-PAGE (10%) was performed and the separated proteins were transferred to 0.45 μm PVDF membrane. The membrane was blocked with 5% skim milk powder at room temperature for 2 h and then incubated with primary antibodies (Abcam, ab128025, ab62557, and ab8245) at 4 °C overnight (1:1000). TBST was used to wash the primary antibodies, and the membranes were incubated with secondary antibodies (ZSGB-BIO, ZB-2301) at room temperature for 60 min. Hypersensitive Electrochemiluminescence liquid (ECL) (Bridgen, D064) was used for visualization. ImageJ software was used to analyze the gray values. The expression levels of LC3 and Beclin-1 are presented as ratios to those of GAPDH.

Table 2 Sequences for primers

Gene	q-PCR
miR-762	Forward 5-ATATATA GGGGCTGGGGCCG-3
	Reverse 5-CAGTGCGTGTCGTGGAGT-3
U6	Forward 5-CTCGCTTCGGCAGCACA-3
	Reverse 5-AACGCTTCACGAATTTGCGT-3
ANP	Forward 5-ACGCAGCTTGGTCACATTGC-3
	Reverse 5-CCACTAGACCACTCATCTAC-3
β-MHC	Forward 5-CTGGCACCGTGGACTACAAC-3
	Reverse 5-CGCACAAAGTGAGGATAGGGT-3
Beclin-1	Forward 5-CGTACAGGATGGACGTGGAG-3
	Reverse 5-GGCAAGACCCCACTTGAGAT-3
GAPDH	Forward 5-AGGTCGGTGTGAACGGATTTG-3
	Reverse 5-TGTAGACCATGTAGTTGAGGTCA-3
miR-762 mimic	5-GGGGCTGGGGCCGGGGCCGAGC-3
miR-762 mimic NC	5-UCACAACCUCCUAGAAAGAGUAGA-3
miR-762 inhibitor	5-CCCCGACCCCGGCCCCGGCUCG-3
miR-762 inhibitor NC	5-CAGUACUUUUGUGUAGUACAAA-3

Transmission electron microscopy

Heart sections (1 m^3) were fixed with 2.5% glutaraldehyde (Solarbio, P1126) and fixed again with 1% osmic acid followed by dehydration with alcohol. Ultrathin sections were made after the samples were embedded in epoxy resin. Quantitative analysis of autophagic vacuoles was carried out using ten images from different fields by an investigator blinded to the origin of each image. Autophagic vacuoles or autolysosomes were identified by characteristic double- or multilamellar smooth membranes completely surrounding compressed mitochondria or by membrane-bound electron-dense material. Electron microscopy (Hitachi, HT7700) was performed at a magnification of ×10,000.

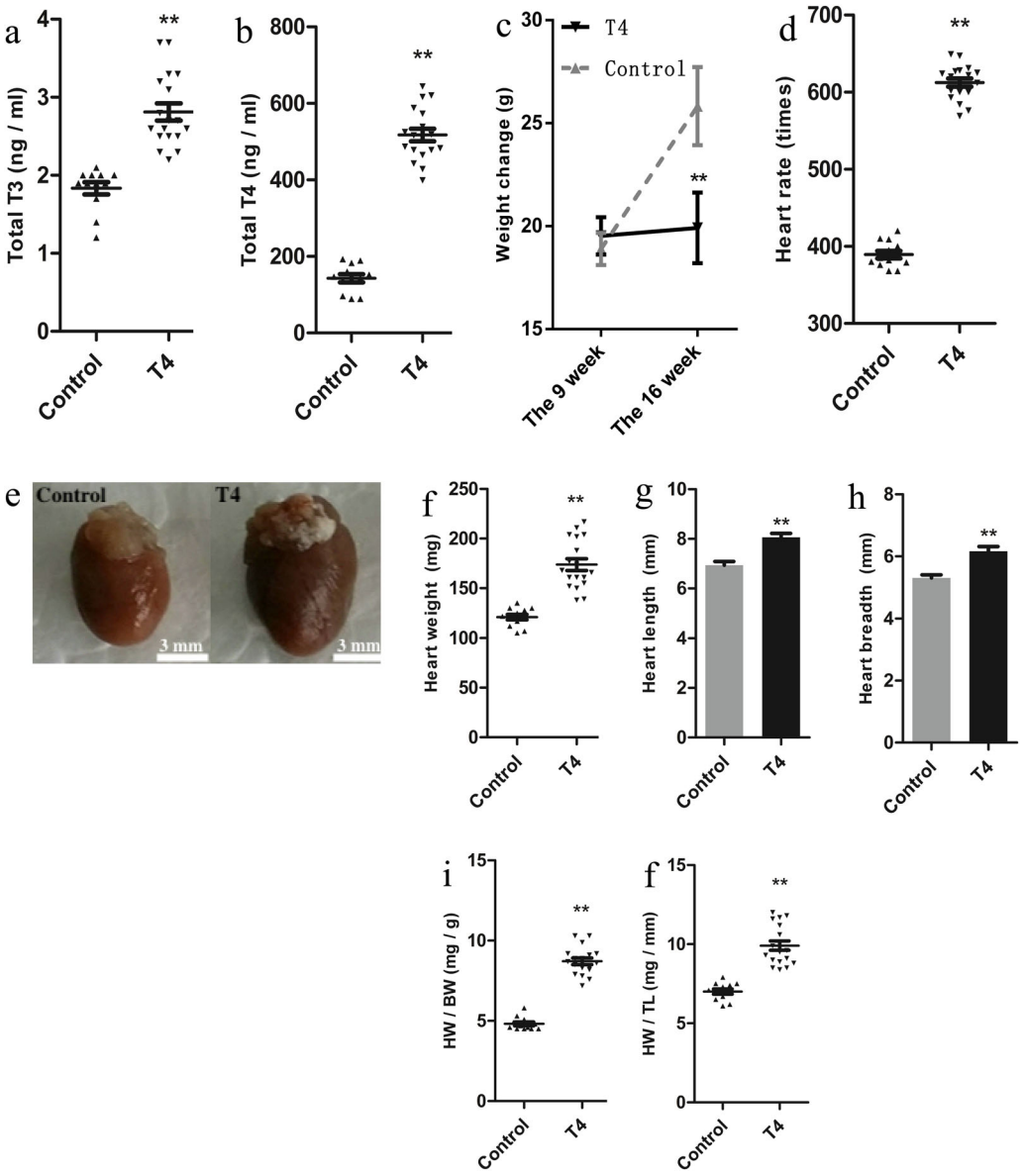

Fig. 1 Intraperitoneal injection of thyroxine successfully induces cardiomyocyte hypertrophy. **a** Serum TT3 after intraperitoneal injection of normal saline or T4 solution. **b** Serum TT4 after intraperitoneal injection of normal saline and T4 solution. **c** Weight changes from week 9 to week 16. **d** Heart beats per minute. **e** Heart perfusion after draining of blood. **f** Heart weight after draining of blood. **g** Vernier caliper measures the longest vertical diameter of the heart. **h** Vernier caliper measures the widest transverse diameter of the heart. **i** The ratio of heart weight to body weight. **j** The ratio of heart weight to tibia length. (**$P < 0.01$ vs the control group; $n \geq 9$ independent samples for each group)

Immunofluorescence

For the paraffin sections, 5 μm sections were heated at 68 °C for 12 h, and then dewaxed and rehydrated in xylene and gradient alcohol. The sections were incubated with 0.4% Triton X (Solarbio, T8200) at room temperature for 20 min and then boiled in ethylenediamine tetraacetic acid (EDTA) (Solarbio, C1034) to boil for 8 min before being incubated in 5% goat serum (Solarbio, SL038) at room temperature for 30 min. The sections were then incubated with primary antibodies (Abcam, ab13524 and ab13524) at 4 °C for overnight (1:100). PBS was used to wash away the primary antibodies for incubating the sections with secondary antibodies (Abcam, ab15007 and ab150160) at room temperature for 30 min (1:1000). DAPI (Solarbio, C0065) was used to counterstain the cell nuclei. Anti quenching agent was used to block the sections. For cardiomyocytes, the cells were fixed with 4% paraformaldehyde and then incubated with 0.1% Triton X-100 for 30 min. Subsequently, the cardiomyocytes were stained with a Cell Navigator F-Actin

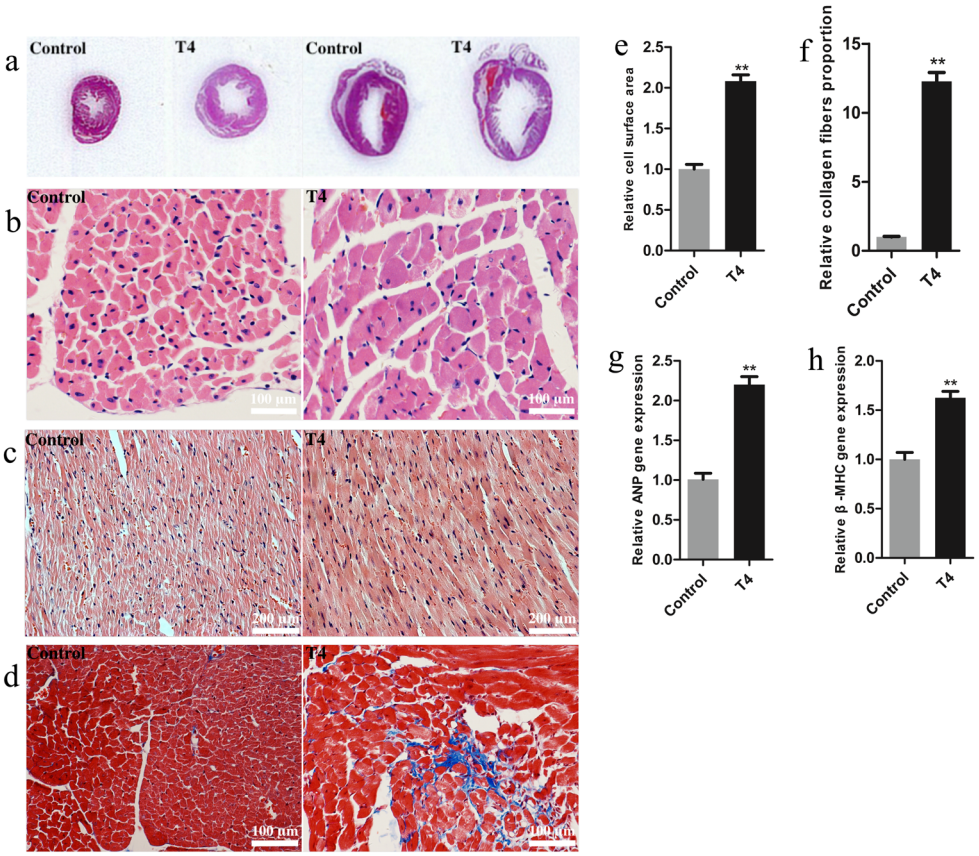

Fig. 2 Intraperitoneal injection of thyroxine successfully induces cardiomyocyte hypertrophy. **a** HE staining showing the outline of the heart. **b** HE staining of myocardial cross section. The cell nuclei are purple, and the cytoplasm is pink, ×400. **c**. HE staining of a myocardial longitudinal section, ×200. **d** Masson staining of a myocardial cross section. Myocardial fibers are red, and collagen fibers are blue, ×400. **e** Semiquantitative analysis of cardiomyocyte surface area in HE-stained sections. **f** The relative proportion of blue collagen fibers as revealed by Masson staining. **g** Semiquantitative analysis of ANP gene expression in the heart. **h** Semiquantitative analysis of β-MHC expression gene in the heart. (**$P < 0.01$ vs the control group; $n \geq 9$ independent samples for each group)

Kit (AAT Bioquest, AAT-22661). Fluorescence microscopy (OLYMPUS, BX53 and FV1000) was performed at magnifications of ×200 and ×2000.

Dual luciferase reporter assay

293A cells were cultured in 24-well plates and transfected with miR-762 mimic negative control (NC) or miR-762 mimic (RiboBio, 50 nM). Twenty-four hours after the initial transfection, the cells were transfected with psiCHECK-2-Beclin-1-3′-UTR-wild type (WT) (Promega, 500 ng) or psiCHECK-2-Beclin-1-3′-UTR- mutant (MU) (Promega, 500 ng) vectors. The 293A cells were lysed, and then the relative luciferase activity was measured with a Dual Luciferase Reporter Assay System (Promega, E1910) on [a] GLOMAXTM 96 microplate luminometer (Promega, E6521). The activity presented as the ratio of Renilla luciferase activity and firefly luciferase activity. Transfection was performed with transfection reagent (RS Biotechnology, CT001).

Cell culture and treatment

Alcohol (75%) was used to disinfect mice within 3 days after birth. The hearts were quickly removed, cut into small pieces, and digested with 0.25% pancreatic enzyme overnight at 4 °C. Serum-free DMEM F12 (HyClone, SH30243.01), 0.1% type II collagenase, and 1% BSA were used to prepare a digestive solution, and then the heart pieces were digested for 10 min at 37 °C. A solution of 10% FBS (Gemini, 9001-108) in DMEM F12 was used to stop the digestion. After centrifugation, the supernatant was discarded, the cells were resuspended in culture medium, and the cell suspension was cultured in CO_2. Finally, the cell suspension was inoculated into a six-well plate at a concentration of 5.0×10^5–1×10^6 cells/ml. The cardiomyocytes were divided into six groups: a control group, a T3 group, a T3 + miR-762 mimic NC group, a T3 + miR-762 mimic group, a T3 + miR-762 inhibitor NC group, and a T3 + miR-762 inhibitor group. The control group was stimulated with DMSO for 24 h, the T3 group was stimulated with T3 solution (15 nM) for 24 h, the T3 + miR-762 mimic NC group was stimulated with the T3 solution and transfected with miR-762 mimic NC (RiboBio, 50 nM) for 24 h, the T3 + miR-762 mimic group was stimulated with the T3 solution and transfected with miR-762 mimic (RiboBio, 50 nM) for 24 h, the T3 + miR-762 inhibitor NC group was stimulated with the T3 solution and transfected with miR-762 inhibitor NC (RiboBio, 100 nM) for 24 h, and the T3 + miR-762 inhibitor group was stimulated with the T3 solution and transfected with miR-762 inhibitor

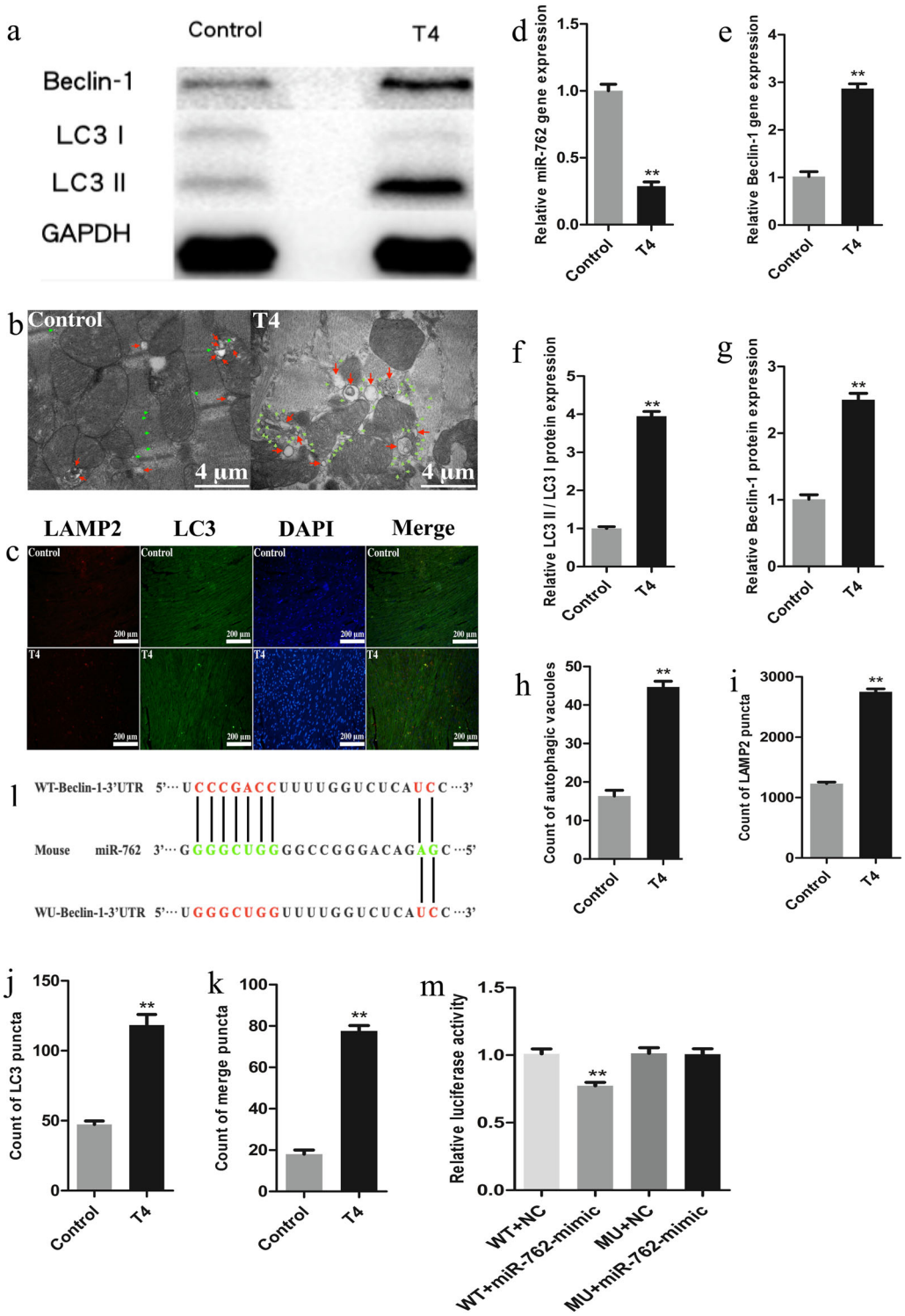

(RiboBio, 100 nM) for 24 h. The T3 solution contained 0.5 g of T3 dissolved in 250 ml of DMSO and was kept protected from light at 4 °C. The transfection process was performed with transfection reagent (RS Biotechnology, CT001).

Statistical analysis

GraphPad Prism 6 software was used to analyze data. All data were expressed as the mean ± SD. Student's *t* test and ANOVA were used to determine statistical significance. For

◀ **Fig. 3** Autophagy plays a key role in thyroxine-induced cardiomyocyte hypertrophy. **a** Expression of LC3 and Beclin-1 protein in the heart. **b** Transmission electron microscopy of the heart. Autophagic vacuoles are green, and autolysosomes are red, ×10,000. **c** Immunofluorescence staining of the heart, LAMP2 protein is red, LC3 protein is green, cell nuclei are blue, and autolysosomes are yellow, ×200. **d** Semiquantitative analysis of miR-762 gene expression in the heart. **e** Semiquantitative analysis of Beclin-1 gene expression in the heart. **f** Semiquantitative analysis of LC3 protein in the heart. **g** Semiquantitative analysis of Beclin-1 protein in the heart. **h** Semiquantitative analysis of autophagic vacuoles with transmission electron microscopy. **i** Semiquantitative analysis of LAMP2 protein with immunofluorescence staining. **j** Semiquantitative analysis of LC3 protein with immunofluorescence staining. **k** Semiquantitative analysis of autolysosomes with immunofluorescence staining. **l** The sequence of the Beclin-1 3′-UTR (http://www.Ensembl.org/) and binding site between miR-762 and Beclin-1 in mice (http://www.Targetscan.org/). **m** Semiquantitative analysis of luciferase activity in 293A cells. (**$P < 0.01$ vs the control group; $n \geq 9$ independent samples for each group)

two-group comparisons, a Student's t test was performed; for comparisons with more than two groups, ANOVA was used. A two-tailed probability value less than 0.05 was considered statistically significant.

Results

Intraperitoneal injection of thyroxine successfully induces cardiomyocyte hypertrophy

Seven weeks after intraperitoneal injection, serum TT3 and TT4 were significantly increased in the T4 group compared with the control group (Fig. 1a, b). There was no significant weight gain in the T4 group, but weight was significantly increased in the control group (Fig. 1c). The mice were anesthetized with 10% chloral hydrate, and then electrocardiography was performed. We found that the control group results were normal, but the heart rate was significantly increased in the T4 group (Fig. 1d). We dissected the hearts and found that compared with those in the control group, the heart weight and volume were significantly increased in the T4 group (Fig. 1e–h). The ratio of heart weight to body weight was also significantly increased in the T4 group (Fig. 1i), as was the ratio of heart weight to tibia length (Fig. 1j). Under the microscope, the cardiomyocyte surface areas in cross sections and vertical sections were significantly increased in the T4 group (Fig. 2a–c, e), and these changes were accompanied by structural disorder and obvious hyperplasia of collagen fibers (Fig. 2d, f). The expression of marker genes of cardiomyocyte hypertrophy, ANP and β-MHC, was significantly upregulated in the T4 group (Fig. 2g, h). These results suggested that an intraperitoneal injection of thyroxine successfully induced cardiomyocyte hypertrophy.

Autophagy plays a key role in thyroxine-induced cardiomyocyte hypertrophy

Compared with that in the control group, the expression of LC3 II/LC3 I and Beclin-1 was significantly upregulated in the T4 group (Fig. 3a, e–g). Under electron microscopy, the number of autophagic vacuoles was significantly increased in the T4 group (Fig. 3b, h). Immunofluorescence also showed that the numbers of lysosomes and autophagic vacuoles were significantly increased in the T4 group (Fig. 3c, i-k). However, the expression of miR-762 was significantly downregulated in the T4 group (Fig. 3d). We found that several nucleotides of miR-762 are perfectly complementary to the Beclin-1 3′-UTR in mice (Fig. 3i). The dual luciferase reporter assay showed that compared with that in the WT + miR-762 mimic NC group, the relative luciferase activity in the WT + miR-762 mimic group was significantly downregulated (Fig. 3m). These results suggest that autophagy plays a key role in thyroxine-induced cardiomyocyte hypertrophy.

miR-762 modulates thyroxine-induced cardiomyocyte hypertrophy by inhibiting Beclin-1

Samples were collected from each group for detection, and the results showed that compared with that in the control group, the cardiomyocyte surface area was significantly increased in the T3 group (Figs. 4a, c and 5a, c). The expression of ANP and β-MHC was also significantly upregulated (Figs. 4f, g and 5f, g). Similarly, LC3 II/LC3 I and Beclin-1 were significantly upregulated in the T3 group (Figs. 4b, e, h, i and 5b, e, h, i). However, the expression of miR-762 was significantly downregulated in the T3 group compared with the control group (Figs. 4d and 5d). In addition, compared with that in the T3 group, the expression of miR-762 was significantly upregulated (Fig. 4d), the cardiomyocyte surface area was significantly decreased in the T3 + miR-762 mimic group (Fig. 4a, c). The expression of ANP and β-MHC was significantly downregulated (Fig. 4f, g), as was that of LC3 II/LC3 I and Beclin-1 in the T3 + miR-762 mimic group compared to the T3 group (Fig. 4b, e, h, i). However, compared with that in the T3 group, the expression of miR-762 was significantly downregulated (Fig. 5d), and the cardiomyocyte surface area was significantly increased in the T3 + miR-762 inhibitor group (Fig. 5a, c). The expression of ANP and β-MHC was significantly upregulated (Fig. 5f, g), as was that of LC3 II/LC3 I and Beclin-1 in the T3 + miR-762 inhibitor group compared to the T3 group (Fig. 5b, e, h, i). These results suggested that miR-762 modulated thyroxine-induced cardiomyocyte hypertrophy by inhibiting Beclin-1.

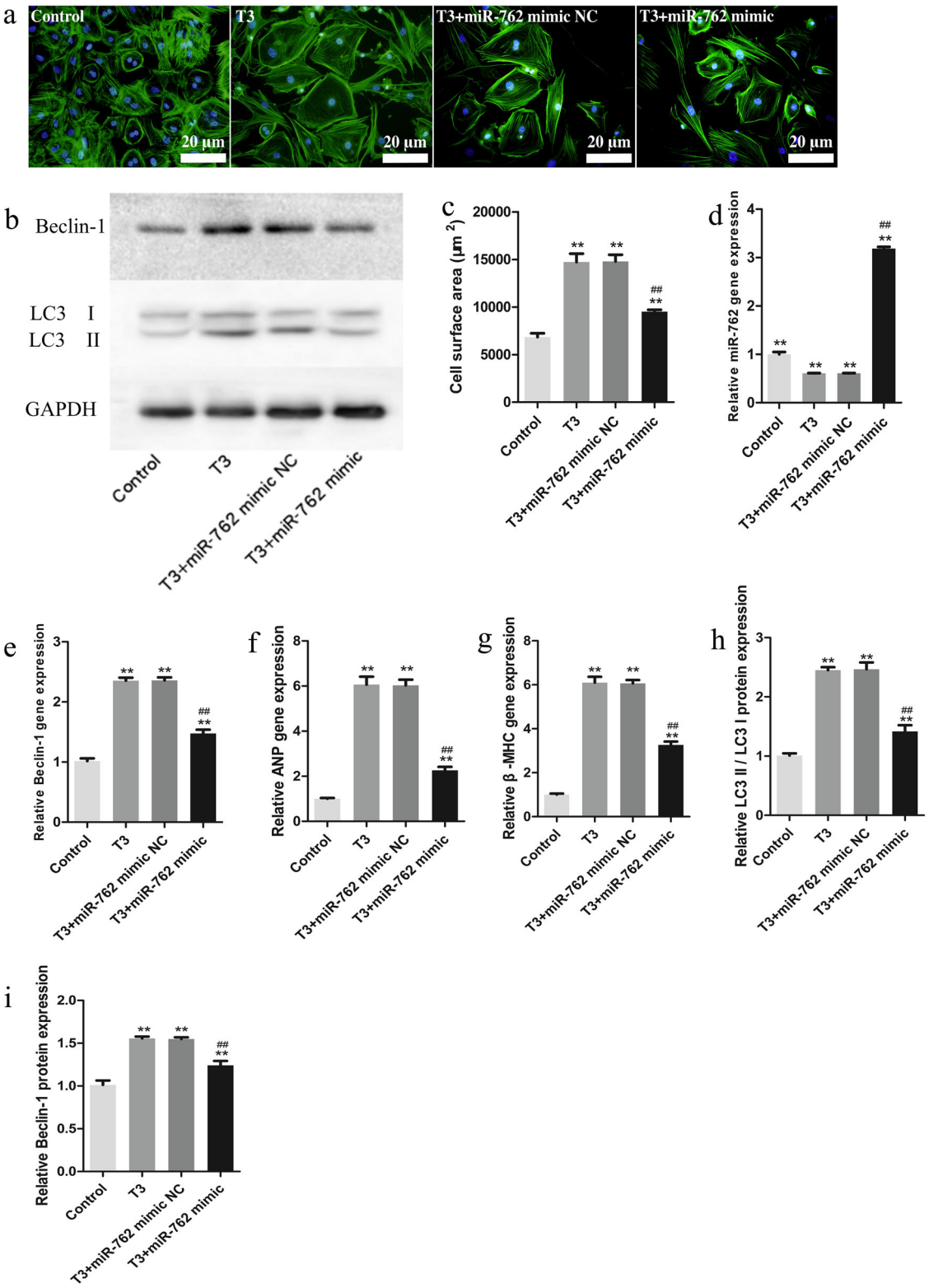

Discussion

In this study, the T4 group was first intraperitoneally injected with T4 solution for 7 weeks, and excessive thyroxine in the blood successfully induced cardiomyocyte hypertrophy. In addition, we found that autophagy was excessively activated in the context of thyroxine-induced cardiomyocyte hypertrophy. Therefore, with

◀ **Fig. 4** miR-762 modulates thyroxine-induced cardiomyocyte hypertrophy by inhibiting Beclin-1. **a** Immunofluorescence staining of cardiomyocytes. Cardiomyocytes are green, and cell nuclei are blue, ×2000. **b** Expression of LC3 and Beclin-1 protein in cardiomyocytes. **c** Surface area of cardiomyocytes as determined by immunofluorescence staining. **d** Semiquantitative analysis of miR-762 gene expression in cardiomyocytes. **e** Semiquantitative analysis of Beclin-1 gene expression in cardiomyocytes. **f** Semiquantitative analysis of ANP gene expression in cardiomyocytes. **g** Semiquantitative analysis of β-MHC gene expression in cardiomyocytes. **h** Semiquantitative analysis of LC3 protein in cardiomyocytes. **i** Semiquantitative analysis of Beclin-1 protein in cardiomyocytes. (**$P < 0.01$ vs the control

regard to our first hypothesis, we confirmed that autophagy plays a key role in thyroxine-induced cardiomyocyte hypertrophy. Subsequently, we used a dual luciferase reporter assay to demonstrate that Beclin-1 is the target gene of miR-762. The results confirmed that miR-762 can regulate autophagy by inhibiting Beclin-1, and provide a basis for future studies on miR-762 and Beclin-1 in the context of thyroxine-induced cardiomyocyte hypertrophy. Finally, the T3 group was stimulated with T3 solution for 24 h, and the results for the T3 group were consistent with the results for the T4 group. Furthermore, the T3 group was treated with miR-762 mimic or inhibitor for 24 h. Cardiomyocyte hypertrophy and autophagic activity were attenuated in the T3 + miR-762 mimic group compared with the T3 group. In contrast, cardiomyocyte hypertrophy and autophagic activity were aggravated in the T3 + miR-762 inhibitor group. More importantly, the expression of Beclin-1 at the mRNA and protein level was opposite to that of miR-762 both in vivo and in vitro. Therefore, with regard to the second hypothesis, we also confirmed that miR-762 modulates thyroxine-induced cardiomyocyte hypertrophy by inhibiting Beclin-1.

Autophagy at basal level is considered to be a protective response under normal physiological conditions. It promotes cell survival by degrading and reusing damaged organelles and proteins, and plays a key role in the turnover of organelles and proteins. Autophagy also participates in normal cell growth and maintains the balance of cardiomyocyte metabolism. However, beyond the range of basal levels, autophagy can be seen as a harmful response associated with states of stress. Excessive autophagy can lead to excessive degradation of organelles and proteins, causing cardiomyocytes to have insufficient amounts of normal organelles and proteins to function, and is not conducive to cardiomyocyte survival [18–20]. In contrast, low autophagy levels can lead to insufficient degradation of organelles and proteins, the turnover of organelles and proteins causing cardiomyocyte metabolism and homeostasis to become unbalanced [21–23]. In summary, after testing the two hypotheses, it is clear that excessive autophagy may be a cause of the occurrence or exacerbation of thyroxine-induced cardiomyocyte hypertrophy. In addition, it is evident that maintaining autophagy levels in the normal range without extreme deviations, may be beneficial for thyroxine-induced cardiomyocyte hypertrophy, and miR-762 may be a good candidate therapeutic target.

It is worth mentioning that miRNAs are similar to hormones: they can be secreted into the blood by cells or tissues, and protected by endogenous RNA enzymes, and they can be stable in the blood [24]. For example, miR-146 is significantly downregulated in Graves' disease patients' plasma, while miR-146 is significantly upregulated in peripheral blood monocytes [25], in addition, miR-146 is significantly upregulated in eye tissue of patients with Graves' disease [26]. These changes are most likely caused by peripheral blood monocytes or eye tissue inhibiting miR-146 release into the plasma. In our results, miR-762 was significantly downregulated in cardiomyocytes and heart tissue; however, miR-762 was previously found to be significantly upregulated in Graves' disease patients' plasma [15]. This upregulation may have been caused by excessive secretion of miR-762 into the plasma by cardiomyocytes or heart tissue.

Although many datasets and results were obtained in our experiment, the limitations of the experiment cannot be ignored. For example, it remains unclear what organelles or proteins are cleared by lysosomes under conditions of excessive autophagy? In addition, the relationship between organelles or proteins deficiency and cardiomyocyte hypertrophy was not elucidated. In this study, we found only that miR-762 modulates thyroxine-induced cardiomyocyte hypertrophy by inhibiting Beclin-1. Therefore, the remaining uncertainties will guide our future research. Another problem that cannot be ignored is that in vivo, the mice were intraperitoneally injected with T4 solution to establish the experimental model. Although this exogenous T4 treatment can simulate hyperthyroidism and significantly increase TT3 and TT4, it can also inhibit the secretion of TSH through negative feedback. Importantly, this decrease in TSH can inhibit the normal differentiation and proliferation of thyroid epithelial cells, and then induce atrophy of the thyroid, ultimately causing the thyroid to produce less thyroxine. However, in most Graves' disease patients is due to the excessive differentiation and proliferation of thyroid epithelial cells. Therefore, we consider our experimental model to be slightly different from clinical patients from Graves' disease in clinical patients, and we will improve our experimental scheme to avoid limitations in future research.

In conclusion, our results reveal that miR-762 modulates thyroxine-induced cardiomyocyte hypertrophy by inhibiting Beclin-1. Importantly, this research helps us better understand the molecular mechanisms of thyroxine-induced cardiomyocyte hypertrophy and establish a theoretical foundation for further research on this condition.

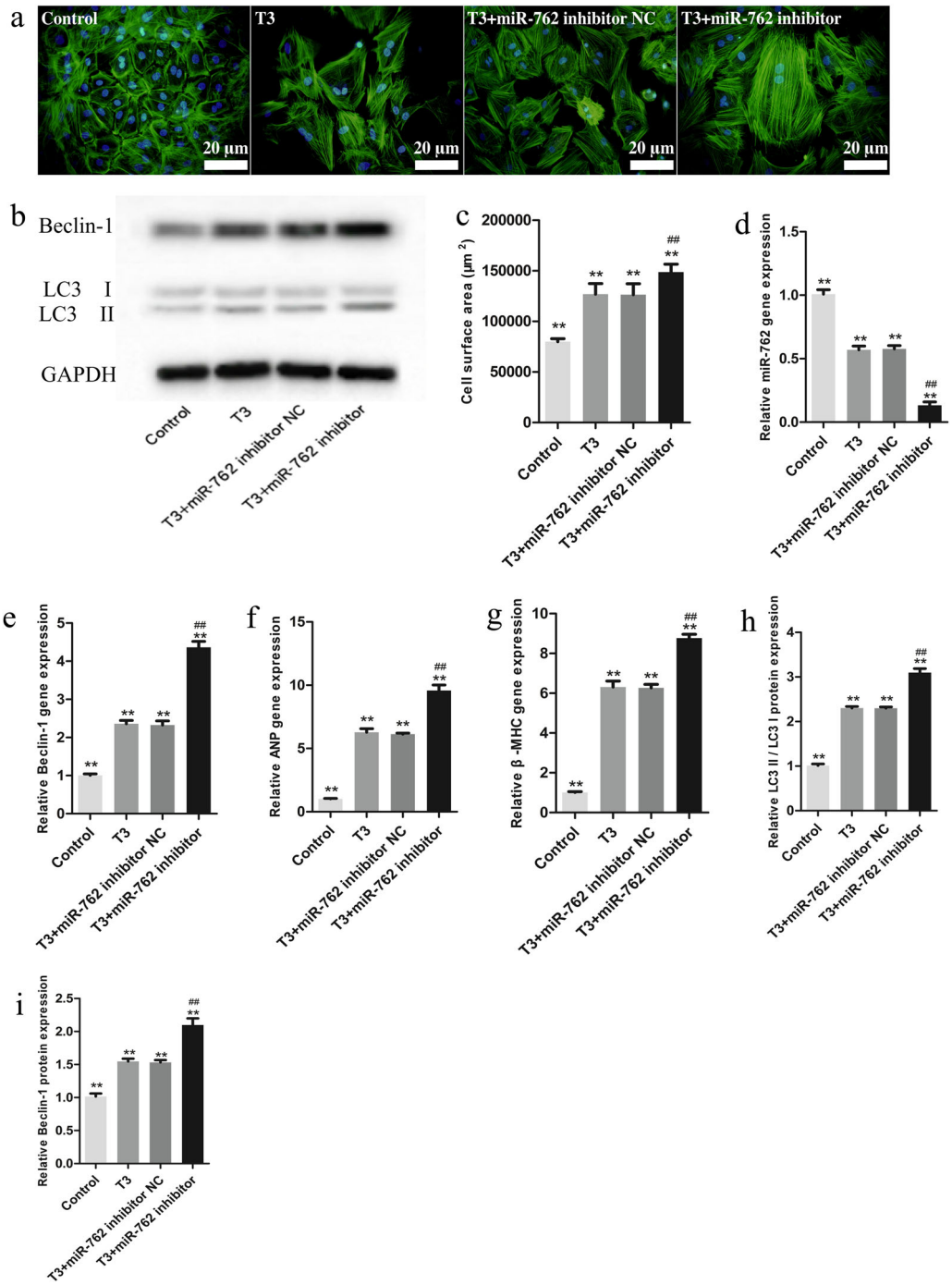

Fig. 5 miR-762 modulates thyroxine-induced cardiomyocyte hypertrophy by inhibiting Beclin-1. **a** Immunofluorescence staining of cardiomyocytes. Cardiomyocytes are green, cell nuclei are blue, ×2000. **b** Expression of LC3 and Beclin-1 protein in cardiomyocytes. **c** Surface area of cardiomyocytes as determined by immunofluorescence staining. **d** Semiquantitative analysis of miR-762 gene expression in cardiomyocytes. **e** Semiquantitative analysis of Beclin-1 gene expression in cardiomyocytes. **f** Semiquantitative analysis of ANP gene expression in cardiomyocytes. **g** Semiquantitative analysis of β-MHC gene expression in cardiomyocytes. **h** Semiquantitative analysis of LC3 protein in cardiomyocytes. **i** Semiquantitative analysis of Beclin-1 protein in cardiomyocytes. (**$P < 0.01$ vs the control group; ##$P < 0.01$ vs the T3 group; $n \geq 9$ independent samples for each group)

Funding The work was supported by the National Natural Science Foundation of China (81660046), the Guangxi Scholarship Fund of the Guangxi Education Department, and the Natural Science Foundation of Guangxi Province (2018GXNSFAA050096).

Compliance with ethical standards

Conflict of interest The authors declare that they have no conflict of interest.

Ethical approval All animal protocols were approved by the review board of the Animal Care and Ethics Committee of Guilin Medical University.

Publisher's note Springer Nature remains neutral with regard to jurisdictional claims in published maps and institutional affiliations.

References

1. R.S. Bahn, H.B. Burch, D.S. Cooper, J.R. Garber, M.C. Greenlee, I. Klein, P. Laurberg, I.R. McDougall, V.M. Montori, S.A. Rivkees, Hyperthyroidism and other causes of thyrotoxicosis: management guidelines of the American Thyroid Association and American Association of Clinical Endocrinologists. Endocr. Pract. **17**(3), 456–520 (2011). https://doi.org/10.14341/ket2011748-18
2. D. Devereaux, S.Z. Tewelde, Hyperthyroidism and thyrotoxicosis. Emerg. Med. Clin. N. Am. **32**(2), 277–292 (2014). https://doi.org/10.1016/j.emc.2013.12.001
3. A.P. Weetman, Graves' disease. N. Engl. J. Med. **343**(17), 1236–1248 (2000). https://doi.org/10.1056/NEJM200010263431707
4. A. Jabbar, A. Pingitore, S.H. Pearce, A. Zaman, Iervasi G., S. Razvi, Thyroid hormones and cardiovascular disease. Nat. Rev. Cardiol. **14**(1), 39–55 (2017). https://doi.org/10.1038/nrcardio.2016.174
5. J. Yuan, H. Liu, W. Gao, L. Zhang, Y. Ye, L. Yuan, Z. Ding, J. Wu, L. Kang, X. Zhang, MicroRNA-378 suppresses myocardial fibrosis through a paracrine mechanism at the early stage of cardiac hypertrophy following mechanical stress. Theranostics **8**(9), 2565–2582 (2018). https://doi.org/10.7150/thno.22878
6. J.P. Wang, R.F. Chi, K. Wang, T. Ma, X.F. Guo, X.L. Zhang, B. Li, F.Z. Qin, X.B. Han, B.A. Fan, Oxidative stress impairs myocyte autophagy, resulting in myocyte hypertrophy. Exp. Physiol. **103**(4), 461–472 (2018). https://doi.org/10.1113/EP086650
7. D. Glick, S. Barth, K.F. Macleod, Autophagy: cellular and molecular mechanisms. J. Pathol. **221**(1), 3–12 (2010). https://doi.org/10.1002/path.2697
8. S. Kaushik, U. Bandyopadhyay, S. Sridhar, R. Kiffin, M. Martinez-Vicente, M. Kon, S.J. Orenstein, E. Wong, A.M. Cuervo, Chaperone-mediated autophagy at a glance. J. Cell Sci. **124**(4), 495–499 (2011). https://doi.org/10.1242/jcs.073874
9. Shuhei Nakamura, Tamotsu Yoshimori, Autophagy and longevity. Mol. Cells **41**(1), 65–72 (2018). https://doi.org/10.14348/molcells.2018.2333
10. Y.Y. Sun, S.S. Qin, Y.H. Cheng, C.Y. Wang, X.J. Liu, Y. Liu, X. L. Zhang, W. Zhang, J.X. Zhan, S. Shao, MicroRNA expression profile and functional analysis reveal their roles in contact inhibition and its disruption switch of rat vascular smooth muscle cells. Acta Pharmacol. Sin. **39**(5), 885–892 (2018). https://doi.org/10.1038/aps.2018.6
11. K. Liu, Q. Hao, J. Wei, G.H. Li, Y. Wu, Y.F. Zhao, MicroRNA-19a/b-3p protect the heart from hypertension-induced pathological cardiac hypertrophy through PDE5A. J. Hypertens. **36**(9), 1847–1857 (2018). https://doi.org/10.1097/HJH.0000000000001769
12. F. Tang, T.L. Yang, MicroRNA-126 alleviates endothelial cells injury in atherosclerosis by restoring autophagic flux via inhibiting of PI3K/Akt/mTOR pathway. Biochem. Biophys. Res. Commun. **495**(1), 1482–1489 (2018). https://doi.org/10.1016/j.bbrc.2017.12.001
13. H. Liu, P. Liu, X. Shi, D. Yin, J. Zhao, NR4A2 protects cardiomyocytes against myocardial infarction injury by promoting autophagy. Cell Death Discov. **4**, 27 (2018). https://doi.org/10.1038/s41420-017-0011-8
14. Y. Li, Y. Wang, M. Zou, C. Chen, Y. Chen, R. Xue, Y. Dong, C. Liu, AMPK blunts chronic heart failure by inhibiting autophagy. Biosci. Rep. **38**(4), BSR20170982 (2018). https://doi.org/10.1042/BSR20170982
15. Q. Yao, X. Wang, W. He, Z. Song, B. Wang, J. Zhang, Q. Qin, Circulating microRNA-144-3p and miR-762 are novel biomarkers of Graves' disease. Endocrine (2019). https://doi.org/10.1007/s12020-019-01884-2.
16. H.H. Samuels, J.S. Tsai, J. Casanova, F. Stanley, Thyroid hormone action: in vitro characterization of solubilized nuclear receptors from rat liver and cultured GH1 cells. J. Clin. Investig. **54**(4), 853–865 (1974). https://doi.org/10.1172/JCI107825
17. P.J. Davis, F.B. Davis, S.A. Mousa, M.K. Luidens, H.Y. Lin, Membrane receptor for thyroid hormone: physiologic and pharmacologic implications. Annu. Rev. Pharmacol. Toxicol. **51**, 99–115 (2011). https://doi.org/10.1146/annurev-pharmtox-010510-100512
18. W. Pan, Y. Zhong, C. Cheng, B. Liu, L. Wang, A. Li, L. Xiong, S. Liu, MiR-30-regulated autophagy mediates angiotensin II-induced myocardial hypertrophy. PLoS ONE **8**(1), e53950 (2013). 10.1371/journal.pone.0053950
19. J. Huang, W. Sun, H. Huang, J. Ye, W. Pan, Y. Zhong, C. Cheng, X. You, B. Liu, L. Xiong, miR-34a modulates angiotensin II-induced myocardial hypertrophy by direct inhibition of ATG9A expression and autophagic activity. PLoS ONE **9**(4), e94382 (2014). 10.1371/journal.pone.0094382
20. A.L. Li, J.B. Lv, L. Gao, MiR-181a mediates Ang II-induced myocardial hypertrophy by mediating autophagy. Eur. Rev. Med. Pharmacol. Sci. **21**(23), 5462–5470 (2017). https://doi.org/10.26355/eurrev20171213936
21. Z. Li, Y. Song, L. Liu, N. Hou, X. An, D. Zhan, Y. Li, L. Zhou, P. Li, L. Yu, miR-199a impairs autophagy and induces cardiac hypertrophy through mTOR activation. Cell Death Differ. **24**(7), 1205–1213 (2017). https://doi.org/10.1038/cdd.2015.95
22. M. Su, J. Wang, C. Wang, X. Wang, W. Dong, W. Qiu, Y. Wang, X. Zhao, Y. Zou, L. Song, MicroRNA-221 inhibits autophagy and promotes heart failure by modulating the p27/CDK2/mTOR axis. Cell Death Differ. **22**(6), 986–999 (2015). https://doi.org/10.1038/cdd.2014.187
23. M. Su, Z. Chen, C. Wang, L. Song, Y. Zou, L. Zhang, R. Hui, J. Wang, Cardiac-specific overexpression of miR-222 induces heart failure and inhibits autophagy in mice. Cell Physiol. Biochem. **39**(4), 1503–1511 (2016). https://doi.org/10.1159/00044785
24. M.A. Cortez, C. Bueso-Ramos, J. Ferdin, G. Lopez-Berestein, A. K. Sood, G.A. Calin, MicroRNAs in body fluids-the mix of hormones and biomarkers. Nat. Rev. Clin. Oncol. **8**(8), 467–477 (2011). https://doi.org/10.1038/nrclinonc.2011.76
25. L. Zheng, C. Zhuang, X. Wang, L. Ming, Serum miR-146a, miR-155, and miR-210 as potential markers of Graves' disease. J. Clin. Lab. Anal. **32**(2) (2018). https://doi.org/10.1002/jcla.22266
26. J. Wang, Y. Xiao, H. Zhang, Role of miR-146a in the Regulation of Inflammation in an In Vitro Model of Graves' orbitopathy. Investig. Ophthalmol. Vis. Sci. **57**(15), 6795 (2016). https://doi.org/10.1167/iovs.16-20559